



ARTICLE

Adaptive Fixed-Time Synchronization of Delayed Memristor-Based Neural Networks with Discontinuous Activations

Tianyuan Jia¹, Xiangyong Chen^{1,2,*}, Xiurong Yao^{1,*}, Feng Zhao¹ and Jianlong Qiu¹

¹School of Automation and Electrical Engineering, and Key Laboratory of Complex Systems and Intelligent Computing in Universities of Shandong, Linyi University, Linyi, 276005, China

²The Hubei Key Laboratory of Advanced Control and Intelligent Automation for Complex Systems, and School of Automation, China University of Geosciences, Wuhan, 430074, China

*Corresponding Authors: Xiangyong Chen. Email: cxy8305@163.com; Xiurong Yao. Email: h190809639@163.com

Received: 11 December 2021 Accepted: 11 February 2022

ABSTRACT

Fixed-time synchronization (FTS) of delayed memristor-based neural networks (MNNs) with discontinuous activations is studied in this paper. Both continuous and discontinuous activations are considered for MNNs. And the mixed delays which are closer to reality are taken into the system. Besides, two kinds of control schemes are proposed, including feedback and adaptive control strategies. Based on some lemmas, mathematical inequalities and the designed controllers, a few synchronization criteria are acquired. Moreover, the upper bound of settling time (ST) which is independent of the initial values is given. Finally, the feasibility of our theory is attested by simulation examples.

KEYWORDS

Memristor-based neural networks; fixed-time synchronization; mixed delays; discontinuous activations; adaptive control

1 Introduction

Memristor is nonlinear resistance having memory function, which represents relationship between magnetic flux and charge. Based on the connections between circuits, Chua proposed the existence of it in 1971 [1]. The first physical memristor is made by Hewlett-Packard Laboratory in 2008 [2]. Unlike ordinary resistors, memristors retain data after a power failure. At present, there are two main applications of memristors: data storage and class brain calculation. Due to the characteristics of small size, low power consumption and fast operation, memristor can be combined with artificial neural networks (NNs) to produce MNNs with more diverse functions and more complex structures. Research on MNNs or NNs have been going on, such as stability [3,4], H_∞ synchronization [5], FTS [6], Mittag-Leffler synchronization [7] and so on.

Due to the chaotic characteristics of MNNs, it appeared in many fields, such as image protection [8] and random number generation [9]. Therefore, the study about synchronization



of MNNs is particularly important. Exponential synchronization of MNNs with impulsive and perturbations were put forward by [10], and given a impulsive controller. Li et al. [11] proposed synchronization within finite-time of BAM MNNs and provided a switching control scheme. FTS of MNNs with fractional order was realized in [12] by using a fractional sliding mode control scheme with no singular terms.

In engineering practice, people always expect the system to realize synchronization as soon as possible. Finite time synchronization attracted people's attention because of its fast error convergence rate and robustness [13,14]. Finite-time synchronization can make the error go to zero for a short time. So many of research on finite-time synchronization. Hua et al. [15] used delay-independent controller to settle synchronization of MNNs with inertial item in finite time without using variable transformation while studying from MNNs themselves. Shi et al. [16] put forward finite-time synchronization of Cohen-Grossberg MNNs and divide error into two states. What needs to be noted is that finite-time synchronization is connected with initial value but it is difficult to acquire for large or complex systems. So this is very limited for applications of finite-time synchronization. While, the limitation was solved by FTS which proposed by [17]. Different from finite-time synchronization, the ST of FTS is not connected with initial values, which greatly improves the application range of FTS in complex dynamical networks [18] and MNNs. So more and more scholars began to study the FTS of MNNs or NNs in recent years. Based on a new proposed lemma, Li et al. [19] realized the fixed time synchronization problem of coupled NNs, and simultaneously the discontinuity and parameters mismatch of the system were considered. And Ren et al. [20] put forward the FTS of stochastic NNs and got the synchronization criteria. Besides, many achievements about FTS of complex-valued and quaternion-valued MNNs or NNs had also been made in [21,22].

The connection weights of MNNs are switchable, so it belongs to a switching system, which is of great significance to the research of switching systems [23]. Meanwhile, it is known that valid control tactics can make the synchronization faster, more stable and easier to meet the needs of practical production applications. Sliding mode control is an effective control method to suppress interference and ensure the stable operation of the nonlinear system [24]. Under the sliding model control method, Xiao et al. [25] realized the FTS of NNs. In addition, with the aid of event-triggered algorithm, Bao et al. [26] studied the synchronization of MNNs. Adaptive control is a resultful control schemes [27,28], it has good robustness and has effective suppression of external interference. Especially when the system has unknown parameters and external disturbance, the adaptive control algorithm can track them, so as to ensure the stable operation of the system. Time delay is universal for nonlinear systems. Especially in engineering practice, when the system signal transmission volume is large, it will lead to channel congestion, resulting in discrete time delay, and when there are parallel channels in the signal transmission path, it will lead to distributed time delay. Time delay will affect the stability of the system and hinder the synchronization of the system. In addition, systems with time delay have complex chaotic characteristics and show complex dynamic behaviors, which are very worthy of study. While some previous literatures [6,12,20,25,26] only considered the constant delay or discrete delay but ignored the distributed delay. For NNs, the activation function realizes the nonlinear transformation of data and solves some problems that the linear model cannot solve. Activation functions are mainly divided into continuous and discontinuous types, but discontinuous activation functions are seldom considered by researchers due to the complexity of analysis.

From above discussion, we find that few people have studied FTS of MNNs, especially the case with mixed delays and discontinuous activation functions. Hence, inspired by above

conditions, the adaptive FTS of delayed MNNs with discontinuous activations are studied in this study. And our contributions are enumerated in following aspects. (1) Complex MNNs model with mixed delay and discontinuous activations is considered. (2) A feedback control scheme and an adaptive control algorithm are proposed for continuous and discontinuous activations, respectively, and the FTS criterion is obtained. Besides, the results are extended to finite-time synchronization. (3) The ST is not affected by the initial value of system and can be adjusted by the controller and system parameters.

2 Model Formulations and Preliminaries

The drive system of MNNs is

$$\begin{aligned} \dot{x}_i(t) = & -z_i x_i(t) + \sum_{j=1}^n k_{ij}(x_i(t)) f_j(x_j(t)) + \sum_{j=1}^n l_{ij}(x_i(t)) g_j(x_j(t - \Delta(t))) \\ & + \sum_{j=1}^n m_{ij}(x_i(t)) \int_{t-w(t)}^t f_j(x_j(s)) ds + I_i. \end{aligned} \tag{1}$$

where $x(t) = (x_1(t), \dots, x_n(t))^T \in R^n$, $z_i > 0$ means rate for i th neuron returns to its idle state and $i, j = 1, 2, \dots, n$. $k_{ij}(\cdot), l_{ij}(\cdot), m_{ij}(\cdot)$ are connection weights. $f_j(\cdot)$ and $g_j(\cdot)$ are activation functions with or without time delay respectively. $\Delta(t)$ delegates discrete time delay and $0 \leq \Delta(t) \leq \Delta_1, 0 \leq \dot{\Delta}(t) \leq \Delta_2 < 1$. $w(t)$ is distributed time delay and $0 \leq w(t) \leq w_1$, where Δ_1, Δ_2, w_1 are constants. $I_i(t)$ is external input vector. The starting condition of (1) is $x_i(s) = \varphi_i(s) \in C([-\tau, 0], R^n)$, $\tau = \max\{\Delta_1, w_1\}$. And $k_{ij}(x_i(t)) = \frac{P'_{ij}}{C_i} \times sign_{ij}, l_{ij}(x_i(t)) = \frac{P'_{ij}}{C_i} \times sign_{ij}, m_{ij}(x_i(t)) = \frac{P''_{ij}}{C_i} \times sign_{ij}$ where $sign_{ij} = 1$ when $i = j$, $sign_{ij} = -1$ when $i \neq j$, and C_i denotes capacitor which voltage is $x_i(t)$. We define the the memristors between $f_j(x_j(t))$ and $x_i(t)$, $g_j(x_j(t - \Delta(t)))$ and $x_i(t)$, $\int_{t-w(t)}^t f_j(x_j(s)) ds$ and $x_i(t)$ are $Q_{ij}, Q'_{ij}, Q''_{ij}$ severally and which resistances are $P_{ij}, P'_{ij}, P''_{ij}$, respectively.

There exist constants $k'_{ij}, k''_{ij}, l'_{ij}, l''_{ij}, m'_{ij}, m''_{ij}$, such that

$$\begin{aligned} k_{ij}(x_i(t)) &= \begin{cases} k'_{ij}, & |x_i(t)| \leq L_j, \\ k''_{ij}, & |x_i(t)| > L_j, \end{cases} \\ l_{ij}(x_i(t)) &= \begin{cases} l'_{ij}, & |x_i(t)| \leq L_j, \\ l''_{ij}, & |x_i(t)| > L_j, \end{cases} \\ m_{ij}(x_i(t)) &= \begin{cases} m'_{ij}, & |x_i(t)| \leq L_j, \\ m''_{ij}, & |x_i(t)| > L_j, \end{cases} \end{aligned}$$

where $K[A]$ denotes the convex closure of the sets A , $\overline{co}[\varepsilon_1, \varepsilon_2]$ is the convex closure generated by real numbers ε_1 and ε_2 , L_j indicates switching threshold and $L_j > 0$. Due to the solutions to MNNs are in the sense of Filippov, so set-valued mappings and differential inclusions [29] are used to deal with the discontinuity of MNNs.

Recur to set-valued mappings, it acquires

$$K[k_{ij}(x_i(t))] = \begin{cases} k'_{ij}, & |x_i(t)| \leq L_j, \\ \overline{co}\{k_{ij}, k_{ij}^*\}, & |x_i(t)| = L_j, \\ k''_{ij}, & |x_i(t)| > L_j, \end{cases}$$

$$K [l_{ij}(x_i(t))] = \begin{cases} l'_{ij}, & |x_i(t)| \leq L_j, \\ \overline{co} \{ \bar{l}_{ij}, l^*_{ij} \}, & |x_i(t)| = L_j, \\ l''_{ij}, & |x_i(t)| > L_j, \end{cases}$$

$$K [m_{ij}(x_i(t))] = \begin{cases} \bar{m}_{ij}, & |x_i(t)| \leq L_j, \\ \overline{co} \{ \bar{m}_{ij}, m^*_{ij} \}, & |x_i(t)| = L_j, \\ \tilde{m}_{ij}, & |x_i(t)| > L_j, \end{cases}$$

where \overline{co} delegates convex closure, we set $\bar{k}_{ij} = \max \{k'_{ij}, k''_{ij}\}, k^*_{ij} = \min \{k'_{ij}, k''_{ij}\}, \bar{k}_{ij} = \max \{|k'_{ij}|, |k''_{ij}|\}, \bar{l}_{ij} = \max \{l'_{ij}, l''_{ij}\}, l^*_{ij} = \min \{l'_{ij}, l''_{ij}\}, \bar{l}_{ij} = \max \{|l'_{ij}|, |l''_{ij}|\}, \bar{m}_{ij} = \max \{m'_{ij}, m''_{ij}\}, m^*_{ij} = \min \{m'_{ij}, m''_{ij}\}, \bar{m}_{ij} = \max \{|m'_{ij}|, |m''_{ij}|\}.$

If the activation functions are continuous, one can obtain

$$\begin{aligned} \dot{x}_i(t) &\in -z_i x_i(t) + \sum_{j=1}^n K [k_{ij}(x_i(t))] f_j(x_j(t)) + \sum_{j=1}^n K [l_{ij}(x_i(t))] g_j(x_j(t - \Delta(t))) \\ &\quad + \sum_{j=1}^n K [m_{ij}(x_i(t))] \int_{t-w(t)}^t f_j(x_j(s)) ds + I_i, \end{aligned} \tag{2}$$

then we set $\tilde{k}_{ij}(x_i(t)) \in K [k_{ij}(x_i(t))], \tilde{l}_{ij}(x_i(t)) \in K [l_{ij}(x_i(t))], \tilde{m}_{ij}(x_i(t)) \in K [m_{ij}(x_i(t))],$ so (2) is rewritten to

$$\begin{aligned} \dot{x}_i(t) &= -z_i x_i(t) + \sum_{j=1}^n \tilde{k}_{ij}(x_i(t)) f_j(x_j(t)) + \sum_{j=1}^n \tilde{l}_{ij}(x_i(t)) g_j(x_j(t - \Delta(t))) \\ &\quad + \sum_{j=1}^n \tilde{m}_{ij}(x_i(t)) \int_{t-w(t)}^t f_j(x_j(s)) ds + I_i. \end{aligned} \tag{3}$$

There also exist $\hat{k}_{ij}(y_i(t)) \in K [k_{ij}(y_i(t))], \hat{l}_{ij}(y_i(t)) \in K [l_{ij}(y_i(t))], \hat{m}_{ij}(y_i(t)) \in K [m_{ij}(y_i(t))]$ for response system, such that

$$\begin{aligned} \dot{y}_i(t) &= -z_i y_i(t) + \sum_{j=1}^n \hat{k}_{ij}(y_i(t)) f_j(y_j(t)) + \sum_{j=1}^n \hat{l}_{ij}(y_i(t)) g_j(y_j(t - \Delta(t))) \\ &\quad + \sum_{j=1}^n \hat{m}_{ij}(y_i(t)) \int_{t-w(t)}^t f_j(y_j(s)) ds + I_i + u_i(t). \end{aligned} \tag{4}$$

where the $u_i(t)$ will be introduced below and starting value of (4) is $y_i(s) = \phi_i(s) \in C([- \tau, 0], \mathbb{R}^n).$

The error is $e_i(t) = y_i(t) - x_i(t),$ so we have

$$\dot{e}_i(t) = -z_i e_i(t) + \sum_{j=1}^n \hat{F}_{ij}(t) + \sum_{j=1}^n \hat{G}_{ij}(t) + \sum_{j=1}^n \tilde{F}_{ij}(t), \tag{5}$$

where $\hat{F}_{ij}(t) = \hat{k}_{ij}(y_i(t)) f_j(y_j(t)) - \tilde{k}_{ij}(x_i(t)) f_j(x_j(t)), \hat{G}_{ij}(t) = \hat{l}_{ij}(y_i(t)) g_j(y_j(t - \Delta(t))) - \tilde{l}_{ij}(x_i(t)) g_j(x_j(t - \Delta(t))), \tilde{F}_{ij}(t) = \hat{m}_{ij}(y_i(t)) \int_{t-w(t)}^t f_j(y_j(s)) ds - \tilde{m}_{ij}(x_i(t)) \int_{t-w(t)}^t f_j(x_j(s)) ds.$

If activation functions are discontinuous, we set $\check{f}_j(x_j) \in K[f_j(x_j)], \check{g}_j(x_j) \in K[g_j(x_j)], \hat{f}_j(y_j) \in K[f_j(y_j)], \hat{g}_j(y_j) \in K[g_j(y_j)]$.

The error is calculated as

$$\dot{e}_i(t) = -z_i e_i(t) + \sum_{j=1}^n F_{ij}^*(t) + \sum_{j=1}^n G_{ij}^*(t) + \sum_{j=1}^n F_{ij}^{**}(t), \tag{6}$$

where $F_{ij}^*(t) = \hat{k}_{ij}(y_i(t))\hat{f}_j(y_j(t)) - \check{k}_{ij}(x_i(t))\check{f}_j(x_j(t))$, $G_{ij}^*(t) = \hat{l}_{ij}(y_i(t))\hat{g}_j(y_j(t - \Delta(t))) - \check{l}_{ij}(x_i(t))\check{g}_j(x_j(t - \Delta(t)))$, $F_{ij}^{**}(t) = \hat{m}_{ij}(y_i(t)) \int_{t-w(t)}^t \hat{f}_j(y_j(s)) ds - \check{m}_{ij}(x_i(t)) \int_{t-w(t)}^t \check{f}_j(x_j(s)) ds$.

Definition 1. [30] For any original value, the FTS of MNNs will be attained if the ST function $T(e_0(s))$ satisfies

$$\lim_{t \rightarrow T(e_0(s))} \|e(t)\| = 0; \|e(t)\| = 0, \forall t \geq T(e_0(s));$$

$$T(e_0(s)) \leq T_{\max}.$$

where T_{\max} is a constant.

Lemma 1. [31] (1) and (4) will attain FTS if a continuous radically unbounded function $V(\cdot): R^n \rightarrow R_+ \cup \{0\}$ satisfies

$$(i) V(c) = 0 \Leftrightarrow c = 0,$$

$$(ii) \dot{V}(c(t)) \leq -d_1 V^{r_1}(c(t)) - d_2 V^{r_2}(c(t)) \text{ for any solution } c(t).$$

where $d_1 > 0, d_2 > 0, 0 < r_1 < 1, r_2 > 1$. And the ST is calculated as

$$T(c_0) \leq T_{\max} = \frac{1}{d_1(1-r_1)} + \frac{1}{d_2(r_2-1)}, \forall c_0 \in R^n.$$

Lemma 2. [32] There are some inequalities as follows:

$$\sum_{i=1}^n p_i^{\vartheta_1} \geq \left(\sum_{i=1}^n p_i\right)^{\vartheta_1}, \sum_{i=1}^n p_i^{\vartheta_2} \geq n^{1-\vartheta_2} \left(\sum_{i=1}^n p_i\right)^{\vartheta_2},$$

where $p_i > 0, 0 < \vartheta_1 \leq 1, \vartheta_2 > 1$.

3 Main Results

The FTS of MNNs with continuous and discontinuous activations will be studied in this section.

3.1 The Continuous Activations for FTS of MNNs

Lemma 3. [33] If $\forall \tilde{k}_{ij}(x) \in K[k_{ij}(x)], \forall \tilde{l}_{ij}(x) \in K[l_{ij}(x)], \forall \hat{k}_{ij}(y) \in K[k_{ij}(y)], \forall \hat{l}_{ij}(y) \in K[k_{ij}(y)]$, the following inequalities are obtained

$$\begin{aligned} \left| \hat{k}_{ij}(y) f_j(y) - \tilde{k}_{ij}(x) f_j(x) \right| &\leq \tilde{k}_{ij} h_j |y - x|, \\ \left| \hat{l}_{ij}(y) g_j(y(t - \Delta(t))) - \tilde{l}_{ij}(x) g_j(x(t - \Delta(t))) \right| &\leq \tilde{l}_{ij} \rho_j |y(t - \Delta(t)) - x(t - \Delta(t))|. \end{aligned}$$

where h_j, ρ_j are constants.

To realize FTS, control algorithm is given as

$$u_i(t) = -\mu_{1i} e_i(t) - \text{sign}(e_i(t)) \left(\mu_{2i} + \mu_{3i} |e_i(t)|^\alpha + \mu_{4i} |e_i(t)|^\beta + \sum_{j=1}^n \mu_{5i} |e_j(t - \Delta(t))| \right), \tag{7}$$

where μ_{1i} to μ_{5i} are constants, $\text{sign}(\cdot)$ is standard sign function and $0 < \alpha < 1, \beta > 1$.

Theorem 1. Under the above assumptions and control scheme (7), the FTS of (1) and (4) will be carried out if the following conditions hold

$$\begin{cases} \mu_{1i} \geq \sum_{j=1}^n \left(\frac{\tilde{k}_{ij} + \tilde{k}_{ij} h_j^2}{2} \right) - z_i, \\ \mu_{2i} \geq 2 \sum_{j=1}^n \tilde{m}_{ij} w_{1j} \tilde{f}_j, \\ \mu_{5i} \geq \max_{1 \leq j \leq n} \left(\tilde{l}_{ij} \rho_j \right). \end{cases} \tag{8}$$

and it can obtain

$$T_1 \leq \frac{2}{q_1(1 - \alpha)} + \frac{2}{(\beta - 1)q_2}, \tag{9}$$

where $q_1 = \min_{1 \leq i \leq n} \{\mu_{3i}\} 2^{\frac{\alpha+1}{2}}, q_2 = \min_{1 \leq i \leq n} \{\mu_{4i}\} n^{\frac{1-\beta}{2}} 2^{\frac{\beta+1}{2}}$.

Proof. Construct Lyapunov function as

$$V(t) = \frac{1}{2} \sum_{i=1}^n e^T(t) e(t). \tag{10}$$

Along the error system (5), the derivative of (10) can be obtained as

$$\begin{aligned} \dot{V}(t) = \sum_{i=1}^n e^T(t) & \left[-z_i e_i(t) + \sum_{j=1}^n \hat{F}_{ij}(t) + \sum_{j=1}^n \hat{G}_{ij}(t) + \sum_{j=1}^n \tilde{F}_{ij}(t) \right. \\ & \left. - \text{sign}(e_i(t)) (\mu_{1i} + \mu_{2i} |e_i(t)| + \mu_{3i} |e_i(t)|^\alpha + \mu_{4i} |e_i(t)|^\beta + \sum_{j=1}^n \mu_{5i} |e_j(t - \Delta(t))|) \right] \end{aligned} \tag{11}$$

By means of Assumption 1 and Lemma 3, we yield

$$\begin{aligned} \sum_{i=1}^n e^T(t) \sum_{j=1}^n \hat{F}_{ij}(t) &\leq \sum_{i=1}^n |e_i(t)| \sum_{j=1}^n \overleftarrow{k}_{ij} h_j |e_j(t)| \\ &\leq \sum_{i=1}^n \sum_{j=1}^n \frac{\overleftarrow{k}_{ij} |e_i(t)|^2}{2} + \sum_{i=1}^n \sum_{j=1}^n \frac{\overleftarrow{k}_{ij} h_j^2 |e_j(t)|^2}{2}, \end{aligned} \tag{12}$$

and

$$\begin{aligned} \sum_{i=1}^n e^T(t) \sum_{j=1}^n \hat{G}_{ij}(t) &\leq \sum_{i=1}^n |e_i(t)| \sum_{j=1}^n \overleftarrow{l}_{ij} \rho_j |e_j(t - \Delta(t))| \\ &\leq \sum_{i=1}^n \sum_{j=1}^n \overleftarrow{l}_{ij} \rho_j |e_i(t)| |e_j(t - \Delta(t))|, \end{aligned} \tag{13}$$

One can also get

$$\sum_{i=1}^n e^T(t) \sum_{j=1}^n \tilde{F}_{ij}(t) \leq 2 \sum_{i=1}^n \sum_{j=1}^n \tilde{m}_{ij} w_1 \bar{f}_j |e_i(t)|. \tag{14}$$

Substitute (12)–(14) into (11), we have

$$\begin{aligned} \dot{V}(t) &\leq \sum_{j=1}^n \{ [-z_i + \sum_{j=1}^n \frac{\overleftarrow{k}_{ij} + \overleftarrow{k}_{ij} h_j^2}{2} - \mu_{1i}] e_i^2(t) \\ &\quad + (2 \sum_{j=1}^n \tilde{m}_{ij} w_1 \bar{f}_j - \mu_{2i}) |e_i(t)| + \sum_{j=1}^n (\overleftarrow{l}_{ij} \rho_j - \mu_{5i}) |e_i(t)| |e_j(t - \Delta(t))| \\ &\quad - \mu_{3i} |e_i(t)|^{\alpha+1} - \mu_{4i} |e_i(t)|^{\beta+1} \}. \end{aligned} \tag{15}$$

According to Throrem 1 and Lemma 2, it has

$$\begin{aligned} \dot{V}(t) &\leq - \sum_{i=1}^n \mu_{3i} |e_i(t)|^{\alpha+1} - \sum_{i=1}^n \mu_{4i} |e_i(t)|^{\beta+1} \\ &\leq - \min_{1 \leq i \leq n} \{ \mu_{3i} \} 2^{\frac{\alpha+1}{2}} (V(t))^{\frac{\alpha+1}{2}} - \min_{1 \leq i \leq n} \{ \mu_{4i} \} 2^{\frac{\beta+1}{2}} n^{\frac{1-\beta}{2}} 2^{\frac{\beta+1}{2}} (V(t))^{\frac{\beta+1}{2}} \\ &= -q_1 (V(t))^{\frac{\alpha+1}{2}} - q_2 (V(t))^{\frac{\beta+1}{2}}, \end{aligned} \tag{16}$$

where $q_1 = \min_{1 \leq i \leq n} \{ \mu_{3i} \} 2^{\frac{\alpha+1}{2}}$, $q_2 = \min_{1 \leq i \leq n} \{ \mu_{4i} \} n^{\frac{1-\beta}{2}} 2^{\frac{\beta+1}{2}}$, and it yields

$$T_1 \leq \frac{2}{q_1(1-\alpha)} + \frac{2}{(\beta-1)q_2}. \tag{17}$$

Remark 1. Especially, when $\alpha = 1 - \frac{1}{2\delta}$, $\beta = 1 + \frac{1}{2\delta}$, the ST is expressed as

$$T_2 \leq T_{\max} = \frac{\pi \delta}{\sqrt{q_3 q_4 n^{\frac{1-\beta}{2}} 2^{\frac{\alpha+\beta+2}{2}}}}, \tag{18}$$

where $q_3 = \min_{1 \leq i \leq n} \{ \mu_{3i} \}$, $q_4 = \min_{1 \leq i \leq n} \{ \mu_{4i} \}$ and $\delta > 1$.

Corollary 1. Under the below control algorithm, (1) and (4) can reach to finite-time synchronization when Assumption 1 and following conditions hold:

$$u_i(t) = -\kappa_{1i}e_i(t) - \text{sign}(e_i(t)) \left(\kappa_{2i} + \kappa_{3i}|e_i(t)|^{\tilde{\alpha}} + \sum_{j=1}^n \kappa_{4i} |e_j(t - \Delta(t))| \right), \tag{19}$$

and

$$\begin{cases} \kappa_{1i} \geq \sum_{j=1}^n \left(\frac{\bar{k}_{ij} + \bar{k}_{ij} h_j^2}{2} \right) - z_i, \\ \kappa_{2i} \geq 2 \sum_{j=1}^n \bar{m}_{ij} w_{1j} \bar{f}_j, \\ \kappa_{4i} \geq \max_{1 \leq j \leq n} \left(\bar{l}_{ij} \rho_j \right), \end{cases} \tag{20}$$

where κ_{1i} to κ_{4i} are constants and $0 < \tilde{\alpha} < 1$, and it can obtain

$$T_3 = \frac{(V(0))^{\frac{1-\tilde{\alpha}}{2}}}{\min_{1 \leq i \leq n} \{\kappa_{3i}\} 2^{\frac{\tilde{\alpha}+1}{2}} \frac{1-\tilde{\alpha}}{2}}. \tag{21}$$

Remark 2. Unlike the exponential or asymptotic [7–9,27,28] which time to synchronization is long or infinite, the FTS has faster convergence. In addition, the finite-time synchronization[14, 26,30] has a fast convergence rate but relies on initial values of the system greatly. However, the starting values of some large and complex systems are hard to know, but FTS overcomes this problem and it can be used widely.

3.2 The Discontinuous Activations for FTS of MNNs

Assumption 1. $f_v, g_v : R \rightarrow R$ are continuous apart from a countable set of ioslate points $\{\theta_\varepsilon\}$. The left limit $f_v\{\theta_\varepsilon^-\}$ and right limit $f_v\{\theta_\varepsilon^+\}$ of f_v exists. Meanwhile, the left limit $g_v\{\theta_\varepsilon^-\}$ and right limit $g_v\{\theta_\varepsilon^+\}$ of g_v exists, and the discontinuous activations $f_v(\tilde{\lambda}), g_v(\tilde{\lambda})$ saify

$$\begin{aligned} K[f_v(\tilde{\lambda})] &= \left[\min \{f_v(\tilde{\lambda}^-), f_v(\tilde{\lambda}^+)\}, \max \{f_v(\tilde{\lambda}^-), f_v(\tilde{\lambda}^+)\} \right], \\ K[g_v(\tilde{\lambda})] &= \left[\min \{g_v(\tilde{\lambda}^-), g_v(\tilde{\lambda}^+)\}, \max \{g_v(\tilde{\lambda}^-), g_v(\tilde{\lambda}^+)\} \right]. \end{aligned}$$

Assumption 2. There are constants $\gamma_v, \gamma'_v, \varsigma_v, \varsigma'_v$, such that

$$\begin{aligned} \sup \left| \widehat{f}_v(\tilde{\chi}) - \check{f}_v(\tilde{\lambda}) \right| &\leq \gamma_v \left| \tilde{\chi} - \tilde{\lambda} \right| + \varsigma_v, \\ \sup \left| \widehat{g}_v(\tilde{\chi}) - \check{g}_v(\tilde{\lambda}) \right| &\leq \gamma'_v \left| \tilde{\chi} - \tilde{\lambda} \right| + \varsigma'_v, \end{aligned}$$

where $\check{f}_v(\tilde{\lambda}) \in K[f_v(\tilde{\lambda})], \widehat{f}_v(\tilde{\chi}) \in K[f_v(\tilde{\chi})], \check{g}_v(\tilde{\lambda}) \in K[g_v(\tilde{\lambda})], \widehat{g}_v(\tilde{\chi}) \in K[g_v(\tilde{\chi})]$.

According to (6), one can get

$$\begin{aligned} \dot{e}_i(t) = & -z_i e_i(t) + \sum_{j=1}^n \hat{k}_{ij}(y_i(t)) \left[\hat{f}_j(y_j(t)) - \tilde{f}_j(x_j(t)) \right] \\ & + \sum_{j=1}^n \left[\hat{k}_{ij}(y_i(t)) - \tilde{k}_{ij}(x_i(t)) \right] \tilde{f}_j(x_j(t)) \\ & + \sum_{j=1}^n \hat{l}_{ij}(y_i(t)) \left[\hat{g}_j(y_j(t - \Delta(t))) - \tilde{g}_j(x_j(t - \Delta(t))) \right] \\ & + \sum_{j=1}^n \left[\hat{l}_{ij}(y_i(t)) - \tilde{l}_{ij}(x_i(t)) \right] \tilde{g}_j(x_j(t - \Delta(t))) \\ & + \sum_{j=1}^n \left[\hat{m}_{ij}(y_i(t)) \int_{t-w(t)}^t \hat{f}_j(y_j(s)) ds - \tilde{m}_{ij}(x_i(t)) \int_{t-w(t)}^t \tilde{f}_j(x_j(s)) ds \right] + u_i(t). \end{aligned} \tag{22}$$

And the nether control adaptive algorithm is designed to ensure the FTS of MNNs.

$$u_i(t) = -\xi_{1i} e_i(t) - \text{sign}(e_i(t)) \left(\xi_{2i} + \xi_{3i} |e_i(t)|^\alpha + \xi_{4i} |e_i(t)|^\beta + \sum_{j=1}^n \xi_{5i} |e_j(t - \Delta(t))| + \xi_{6i}(t) |e_i(t)| \right), \tag{23}$$

and adaptive law is

$$\dot{\xi}_{6i}(t) = e_i^T(t) e_i(t) - \xi_{3i} (\xi_{6i}(t) - \varpi_1)^\alpha - \xi_{4i} (\xi_{6i}(t) - \varpi_1)^\beta, \tag{24}$$

where $\xi_{6i}(t)$ is adaptive gain, ξ_{1i} to ξ_{5i} and ϖ_1 are constants.

Theorem 2. FTS with discontinuous activations will be attained under Assumptions 3 and 4 and control (24) if following conditions are met.

$$\begin{cases} \xi_{1i} \geq \sum_{j=1}^n \left(\frac{\tilde{k}_{ij} + \tilde{k}_{ij} \gamma_j^2}{2} \right) - z_i - \varpi_1, \\ \xi_{2i} \geq \sum_{j=1}^n \left[\tilde{k}_{ij} \zeta_j + (\tilde{k}_{ij} - k_{ij}^*) \tilde{f}_j + \tilde{l}_{ij} \zeta'_j + (\tilde{l}_{ij} - l_{ij}^*) \tilde{g}_j + 2 \tilde{m}_{ij} w_1 \tilde{f}_j \right], \\ \xi_{5i} \geq \max_{1 \leq j \leq n} (\tilde{l}_{ij} \gamma'_j). \end{cases} \tag{25}$$

Proof. Choose Lyapunov function as

$$V(t) = \frac{1}{2} \left(\sum_{i=1}^n e_i^T(t) e_i(t) + \sum_{i=1}^n (\xi_{6i}(t) - \varpi_1)^2 \right). \tag{26}$$

Take derivative of $V(t)$ along (25), it acquires

$$\begin{aligned}
\dot{V}(t) &= \sum_{i=1}^n e_i^T(t) \dot{e}_i(t) + \sum_{i=1}^n (\xi_{6i}(t) - \varpi_1) \dot{\xi}_{6i}(t) \\
&= \sum_{i=1}^n e_i^T(t) \left\{ -z_i e_i(t) + \sum_{j=1}^n \hat{k}_{ij}(y_i(t)) \left[\widehat{f}_j(y_j(t)) - \widetilde{f}_j(x_j(t)) \right] \right. \\
&\quad + \sum_{j=1}^n \left[\hat{k}_{ij}(y_i(t)) - \widetilde{k}_{ij}(x_i(t)) \right] \widetilde{f}_j(x_j(t)) \\
&\quad + \sum_{j=1}^n \hat{l}_{ij}(y_i(t)) \left[\widehat{g}_j(y_j(t - \Delta(t))) - \widetilde{g}_j(x_j(t - \Delta(t))) \right] \\
&\quad + \sum_{j=1}^n \left[\hat{l}_{ij}(y_i(t)) - \widetilde{l}_{ij}(x_i(t)) \right] \widetilde{g}_j(x_j(t - \Delta(t))) \\
&\quad + \sum_{j=1}^n \left[\hat{m}_{ij}(y_i(t)) \int_{t-w(t)}^t \widehat{f}_j(y_j(s)) ds - \widetilde{m}_{ij}(x_i(t)) \int_{t-w(t)}^t \widetilde{f}_j(x_j(s)) ds \right] \\
&\quad \left. + u_i(t) \right\} + \sum_{i=1}^n (\xi_{6i}(t) - \varpi_1) \left(e_i^T(t) e_i(t) - \xi_{3i} (\xi_{6i}(t) - \varpi_1)^\alpha - \xi_{4i} (\xi_{6i}(t) - \varpi_1)^\beta \right)
\end{aligned} \tag{27}$$

With Assumption 3, it gets

$$\begin{aligned}
&\sum_{i=1}^n e_i^T(t) \sum_{j=1}^n \hat{k}_{ij}(y_i(t)) \left[\widehat{f}_j(y_j(t)) - \widetilde{f}_j(x_j(t)) \right] \\
&\leq \sum_{i=1}^n \sum_{j=1}^n \widetilde{k}_{ij} (\gamma_j |e_j(t)| + \varsigma_j) |e_i(t)| \\
&\leq \sum_{i=1}^n \sum_{j=1}^n \left(\frac{\widetilde{k}_{ij} |e_i(t)|^2 + \widetilde{k}_{ij} \gamma_j^2 |e_i(t)|^2}{2} + \widetilde{k}_{ij} \varsigma_j |e_i(t)| \right),
\end{aligned} \tag{28}$$

and

$$\begin{aligned}
&\sum_{i=1}^n e_i^T(t) \sum_{j=1}^n \hat{l}_{ij}(y_i(t)) \left[\widehat{g}_j(y_j(t - \Delta(t))) - \widetilde{g}_j(x_j(t - \Delta(t))) \right] \\
&\leq \sum_{i=1}^n \sum_{j=1}^n \widetilde{l}_{ij} (\gamma'_j |e_j(t - \Delta(t))| + \varsigma'_j) |e_i(t)| \\
&= \sum_{i=1}^n \sum_{j=1}^n \left(\widetilde{l}_{ij} \gamma'_j |e_i(t)| |e_j(t - \Delta(t))| + \widetilde{l}_{ij} \varsigma'_j |e_i(t)| \right).
\end{aligned} \tag{29}$$

Besides, one can obtain

$$\begin{aligned}
&\sum_{i=1}^n e_i^T(t) \sum_{j=1}^n \left[\hat{k}_{ij}(y_i(t)) - \widetilde{k}_{ij}(x_i(t)) \right] \widetilde{f}_j(x_j(t)) \\
&\leq \sum_{i=1}^n \sum_{j=1}^n \left[\widetilde{k}_{ij} - k_{ij}^* \right] \widetilde{f}_j |e_i(t)|,
\end{aligned} \tag{30}$$

$$\begin{aligned} & \sum_{i=1}^n e_i^T(t) \sum_{j=1}^n \left[\hat{l}_{ij}(y_i(t)) - \tilde{l}_{ij}(x_i(t)) \right] \tilde{g}_j(x_j(t - \Delta(t))) \\ & \leq \sum_{i=1}^n \sum_{j=1}^n \left[\bar{l}_{ij} - l_{ij}^* \right] \bar{g}_j |e_i(t)| \end{aligned} \tag{31}$$

and

$$\begin{aligned} & \sum_{i=1}^n e_i^T(t) \sum_{j=1}^n \left[\hat{m}_{ij}(y_i(t)) \int_{t-w(t)}^t f_j(y_j(s)) ds - \tilde{m}_{ij}(x_i(t)) \int_{t-w(t)}^t f_j(x_j(s)) ds \right] \\ & \leq 2 \sum_{i=1}^n \sum_{j=1}^n \bar{m}_{ij} w_1 \bar{f}_j |e_i(t)| \end{aligned} \tag{32}$$

So it yields

$$\begin{aligned} \dot{V}(t) & \leq \sum_{i=1}^n \left\{ \left[\sum_{j=1}^n \left(\bar{k}_{ij} \zeta_j + (\bar{k}_{ij} - k_{ij}^*) \bar{f}_j + \bar{l}_{ij} \zeta'_j + (\bar{l}_{ij} - l_{ij}^*) \bar{g}_j + 2\bar{m}_{ij} w_1 \bar{f}_j \right) - \xi_{2i} \right] |e_i(t)| \right. \\ & \quad + [-z_i + \sum_{j=1}^n \left(\frac{\bar{k}_{ij} + \bar{k}_{ij} \gamma_j^2}{2} \right) - \varpi_1 - \xi_{1i}] |e_i(t)|^2 \\ & \quad + \sum_{j=1}^n \left(\bar{l}_{ij} \gamma'_j - \xi_{5i} \right) |e_i(t)| |e_j(t - \Delta(t))| - \xi_{3i} |e_i(t)|^{\alpha+1} - \xi_{4i} |e_i(t)|^{\beta+1} \\ & \quad \left. - \xi_{6i}(t) |e_i(t)|^2 + \varpi_1 |e_i(t)|^2 - \xi_{3i} (\xi_{6i}(t) - \varpi_1)^{\alpha+1} - \xi_{4i} (\xi_{6i}(t) - \varpi_1)^{\beta+1} \right. \\ & \quad \left. + (\xi_{6i}(t) - \varpi_1) |e_i(t)|^2 \right\} \end{aligned} \tag{33}$$

According to Theorem 2, it has

$$\begin{aligned} \dot{V}(t) & \leq - \sum_{i=1}^n \xi_{3i} |e_i(t)|^{\alpha+1} - \sum_{i=1}^n \xi_{4i} |e_i(t)|^{\beta+1} \\ & \quad - \sum_{i=1}^n \xi_{3i} (\xi_{6i}(t) - \varpi_1)^{\alpha+1} - \sum_{i=1}^n \xi_{4i} (\xi_{6i}(t) - \varpi_1)^{\beta+1} \\ & \leq - \min_{1 \leq i \leq n} \{ \xi_{3i} \} \left(\sum_{i=1}^n |e_i(t)|^2 + \sum_{i=1}^n (\xi_{6i}(t) - \varpi_1)^2 \right)^{\frac{\alpha+1}{2}}, \\ & \quad - \min_{1 \leq i \leq n} \{ \xi_{4i} \} n^{\frac{1-\beta}{2}} \left(\sum_{i=1}^n |e_i(t)|^2 + \sum_{i=1}^n (\xi_{6i}(t) - \varpi_1)^2 \right)^{\frac{\beta+1}{2}} \\ & = -q_5(V(t))^{\frac{\alpha+1}{2}} - q_6(V(t))^{\frac{\beta+1}{2}} \end{aligned} \tag{34}$$

where $q_5 = \min_{1 \leq i \leq n} \{ \xi_{3i} \} 2^{\frac{\alpha+1}{2}}$, $q_6 = \min_{1 \leq i \leq n} \{ \xi_{4i} \} n^{\frac{1-\beta}{2}} 2^{\frac{\beta+1}{2}}$, and we can get

$$T_4 \leq T_{\max} = \frac{2}{q_5(1-\alpha)} + \frac{2}{q_6(\beta-1)}. \tag{35}$$

Remark 3. If $\alpha = 1 - \frac{1}{2\mu}, \beta = 1 + \frac{1}{2\mu}$, it acquires

$$T_5 \leq T_{\max} = \frac{\pi \mu}{\sqrt{q_7 q_8 n^{\frac{1-\beta}{2}} 2^{\frac{\alpha+\beta+2}{2}}}}, \tag{36}$$

where $q_7 = \min_{1 \leq i \leq n} \{\xi_{3i}\}, q_8 = \min_{1 \leq i \leq n} \{\xi_{4i}\}$ and $\mu > 1$.

Corollary 2. Under Assumptions 3 and 4, (1) and (4) attain finite-time synchronization with control scheme (37) if following conditions hold

$$u_i(t) = -b_{1i}e_i(t) - \text{sign}(e_i(t)) \left(b_{2i} + b_{3i}|e_i(t)|^\alpha + \sum_{j=1}^n b_{4i} |e_j(t - \Delta(t))| + \xi_{6i}(t) |e_i(t)| \right), \tag{37}$$

and adaptive law is

$$\dot{\xi}_{6i}(t) = e_i^T(t) e_i(t) - b_{3i}(\xi_{6i}(t) - \varpi_1)^\alpha, \tag{38}$$

and

$$\begin{cases} b_{1i} \geq \sum_{j=1}^n \left(\frac{\bar{k}_{ij} + \bar{k}_{ij} \gamma_j^2}{2} \right) - z_i - \varpi_1, \\ b_{2i} \geq \sum_{j=1}^n \left[\bar{k}_{ij} \zeta_j + (\bar{k}_{ij} - k_{ij}^*) \bar{f}_j + \bar{l}_{ij} \zeta'_j + (\bar{l}_{ij} - l_{ij}^*) \bar{g}_j + 2\bar{m}_{ij} w_1 \bar{f}_j \right], \\ b_{4i} \geq \max_{1 \leq j \leq n} (\bar{l}_{ij} \gamma'_j), \end{cases} \tag{39}$$

where b_{1i} to b_{4i} are positive constants and $0 < \alpha < 1$ and it acquires

$$T_6 = \frac{(V(0))^{\frac{1-\alpha}{2}}}{\min_{1 \leq i \leq n} \{b_{3i}\} 2^{\frac{\alpha+1}{2}} \frac{1-\alpha}{2}}. \tag{40}$$

Remark 4. Compared with continuous activation functions [20,25], our study considers the more complicated discontinuous activation functions and mixed delays. Besides, it is known that the gain of feedback control is always larger than the practical application, so the adaptive control are used for FTS in this subjection. The adaptive control has robustness, anti-interference and good suppression effect on external interference, even in the case of some unknown system parameters can also achieve good control effect.

Remark 5. The synchronization criteria of FTS and the upper bound of ST are obtained in our study. Besides, we also derive the relevant criteria for finite-time synchronization, which is more comprehensive than the paper that only studies FTS or finite-time synchronization. From (17) and (35), it's pretty obvious that ST does not rely on starting values and can be adjusted by changing controller paramaters: μ_{3i}, μ_{4i} and ξ_{3i}, ξ_{4i} .

4 Numerical Examples

Examples are offered in this section verifying validity and superiority of above theoretical derivation.

Example 1. This example to verify the FTS of MNNs with continuous activations.

Consider drive system of MNNs with two neurons as

$$\begin{aligned} \dot{x}_i(t) = & -z_i x_i(t) + \sum_{j=1}^n k_{ij}(x_i(t)) f_j(x_j(t)) + \sum_{j=1}^n l_{ij}(x_i(t)) g_j(x_j(t - \Delta(t))) \\ & + \sum_{j=1}^n m_{ij}(x_i(t)) \int_{t-w(t)}^t f_j(x_j(s)) ds + I_i. \end{aligned} \tag{41}$$

The weighted matrices are

$$\begin{aligned} K_1 = & \begin{bmatrix} 1.1 & -0.4 \\ 0.8 & -0.7 \end{bmatrix}, K_2 = \begin{bmatrix} 1 & -0.5 \\ 1 & -0.6 \end{bmatrix}, \\ L_1 = & \begin{bmatrix} -0.5 & 0.3 \\ 0.9 & -1.6 \end{bmatrix}, L_2 = \begin{bmatrix} -0.8 & 0.4 \\ 0.7 & -1.7 \end{bmatrix}, \\ M_1 = & \begin{bmatrix} -1.3 & 0.2 \\ -0.6 & 0.5 \end{bmatrix}, M_2 = \begin{bmatrix} -1.5 & 0.4 \\ -0.4 & 0.8 \end{bmatrix}. \end{aligned}$$

$$\begin{aligned} \dot{y}_i(t) = & -z_i y_i(t) + \sum_{j=1}^n k_{ij}(y_i(t)) f_j(y_j(t)) + \sum_{j=1}^n l_{ij}(y_i(t)) g_j(y_j(t - \Delta(t))) \\ & + \sum_{j=1}^n m_{ij}(y_i(t)) \int_{t-w(t)}^t f_j(y_j(s)) ds + I_i. \end{aligned} \tag{42}$$

where $i, j = 1, 2$, the switching threshold $L_j = 1$. The delays are set as $\Delta(t) = \sin(t)$ and $w(t) = \frac{e^t}{e^t + 1}$. The starting values are select as $x_i(t) = [-4, -2]^T, y_i(t) = [3, 2]^T$. And the $f_j(\cdot) = g_j(\cdot) = \tanh(\cdot)$.

To attain FTS, the parameters are selected as $\rho_1 = \rho_2 = 1, h_1 = h_2 = 1, z_1 = z_2 = 1, \mu_{11} = 3.40, \mu_{12} = 1.60, \mu_{21} = 0.20, \mu_{22} = 1.60, \mu_{31} = 1.2, \mu_{32} = 1, \mu_{41} = 1.6, \mu_{42} = 1.2, \mu_{51} = 1.5, \mu_{52} = 0.8, \alpha = 0.5, \beta = 1.5, f_j = \bar{g}_j = 1, w_1 = 1$.

The chaotic trajectory with control is shown in Fig. 1. Under the action of the controller, the chaotic orbits of the driving system $y_1(t), y_2(t)$ finally converge with those of the response system $x_1(t), x_2(t)$, that is, the synchronization is realized. The curves of states and errors with control algorithm are exhibited in Figs. 2 to 4. The synchronization curves of states $x(t)$ and $y(t)$ are shown in Figs. 2 and 3. It can be seen from the figures that the synchronization of the two states is realized within a finite-time under the action of the control scheme. Fig. 4 illustrates that the errors $e_1(t)$ and $e_2(t)$ approach 0 under the action of the controller, i.e., finite-time synchronization is achieved.

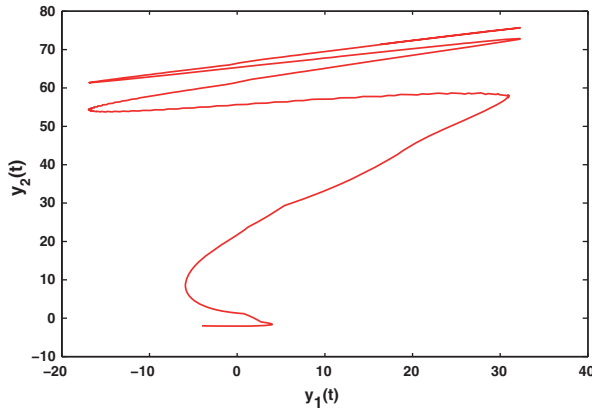


Figure 1: The phase plot of (42) with control

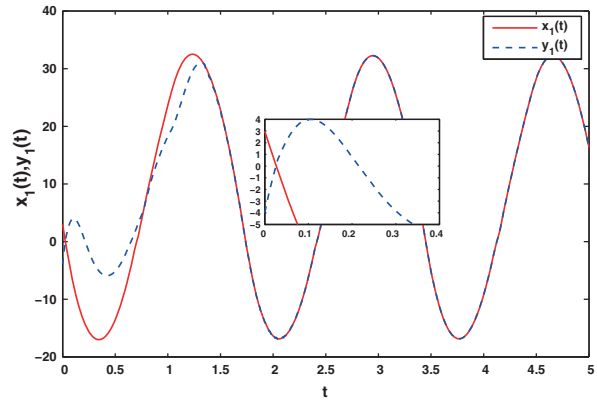


Figure 2: The state diagrams with control

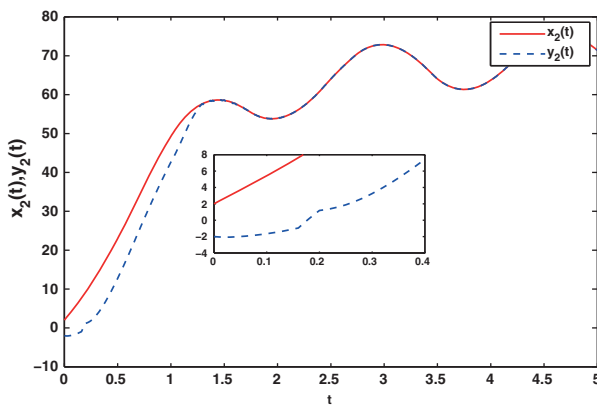


Figure 3: The state diagrams with control

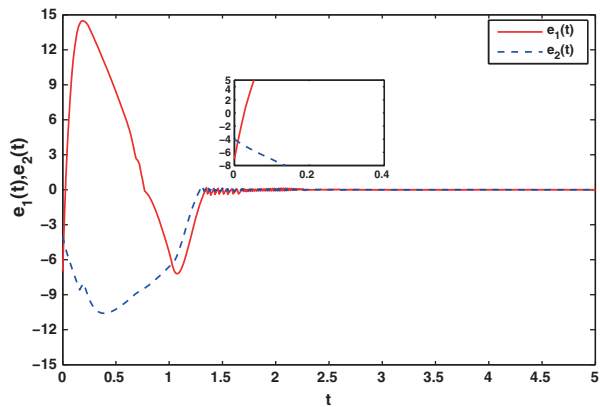


Figure 4: The error graphs with control

Example 2. This example to illustrate the FTS of MNNs with discontinuous activations.

The initial values are set as $x_i(t) = [-5, -3]^T, y_i(t) = [5, 4]^T$. And the $f_j(\cdot) = g_j(\cdot) = 0.8 \tanh(\cdot) + 0.04 \text{sign}(\cdot)$. The switching threshold and mixed delays are same to example 1. If the controller are added into the error system and the relevant parameters are selected as $\gamma_1 = \gamma_2 = \gamma'_1 = \gamma'_2 = 0.9, \varsigma_1 = \varsigma_2 = \varsigma'_1 = \varsigma'_2 = 0.03, \varpi_1 = 2, \xi_{11} = 3.8670, \xi_{12} = 3.0690, \xi_{21} = -1.4615, \xi_{22} = -1.4615, \xi_{31} = 1.5, \xi_{32} = 1.7, \xi_{41} = 2, \xi_{42} = 2.4, \bar{f}_j = 0.84$, and the system can achieve synchronization. The corresponding synchronous plots are shown in Figs. 10 to 14.

Fig. 5 shows the chaotic trajectory of the driving system, and Fig. 6 shows the chaotic trajectory of the response system without the action of the controller. It can be found that the curves in the two pictures are different. The chaos diagram of the response system under the action of the controller can be seen in Fig. 10. It can be found that Fig. 10 is consistent with Fig. 5.

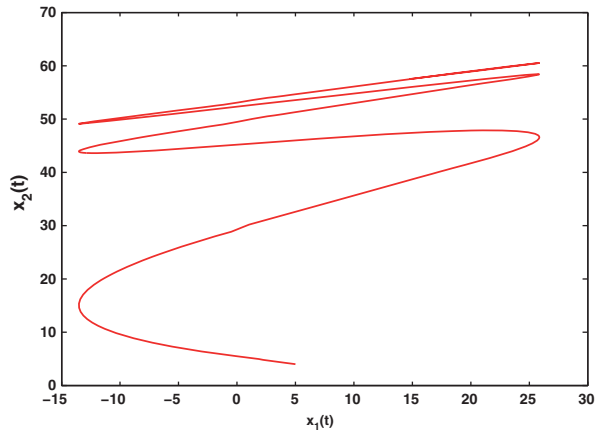


Figure 5: The phase plot of MNNs (41)

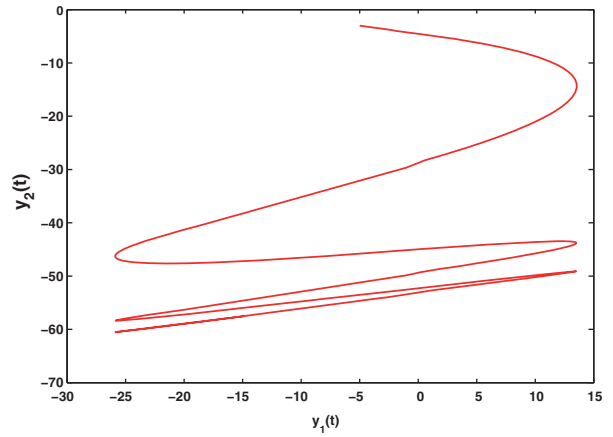


Figure 6: The phase plot of MNNs (42)

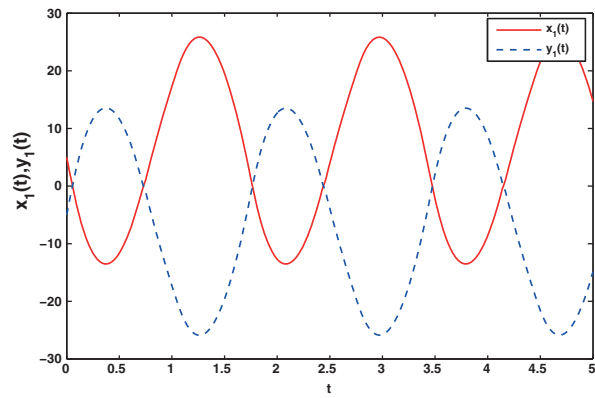


Figure 7: The state graphs without control

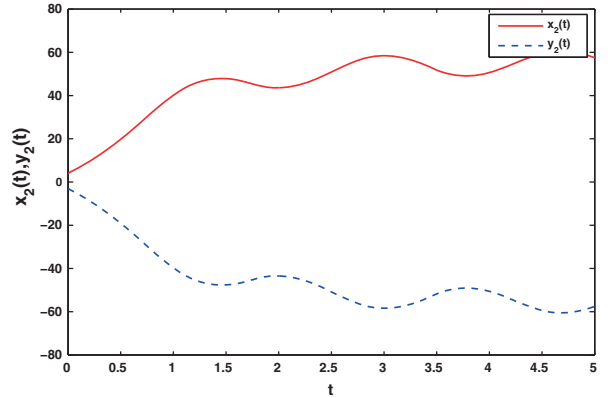


Figure 8: The state graphs without control

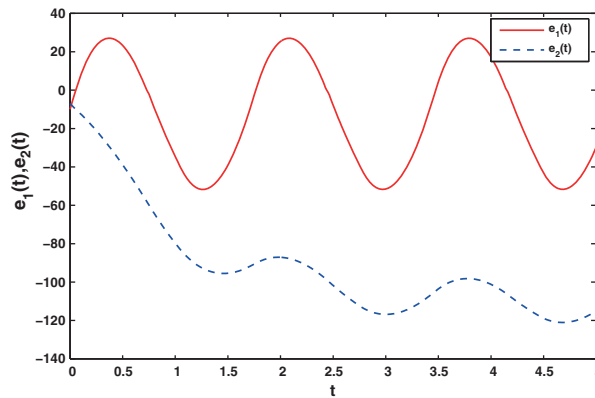


Figure 9: The error graphs without control

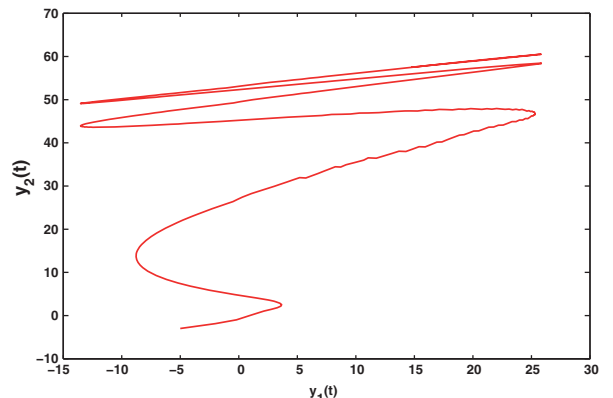


Figure 10: The phase plot of (42) with control

Figs. 7 to 9 show the state curves and error curves without the action of the controller. It can be found that the curves are not synchronized. Under the action of the adaptive control algorithm, Figs. 11 and 12 show that the state trajectories of the drive and response system realize finite-time synchronization, and Fig. 13 shows that the system errors eventually approach to zero. In addition, the evolution curves of adaptive gains for the proposed adaptive control scheme are shown in Fig. 14.

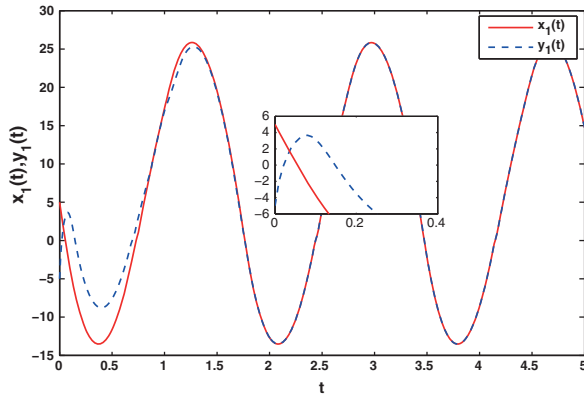


Figure 11: The state graphs with control

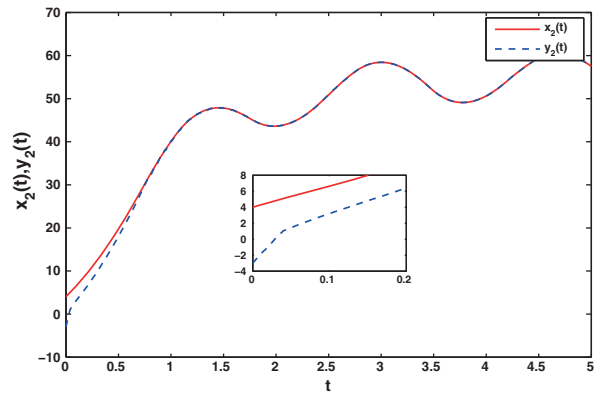


Figure 12: The state graphs with control

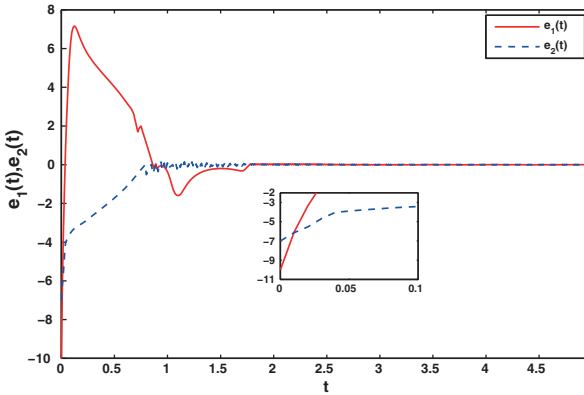


Figure 13: The error graphs with control

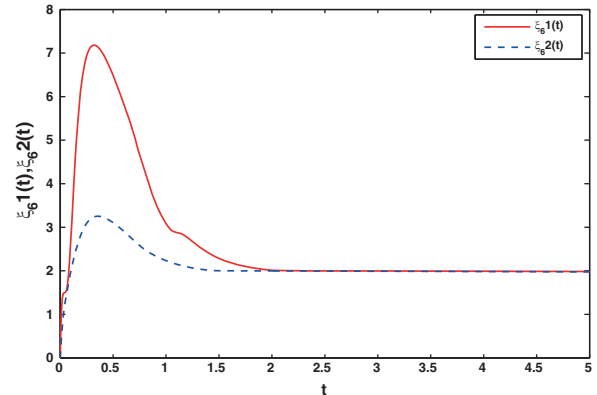


Figure 14: The evolutions of adaptive gain

5 Conclusions

The FTS of delayed MNNs with two kinds of activations are discussed. A feedback control algorithm is given for continuous activations and an adaptive control scheme is given for discontinuous activations. Besides, the Filippov theory is used to solve the noncontinuity of MNNs and obtain the synchronization criteria. In addition, through formula derivation, we also draw the conclusion of finite-time synchronization under the same model, so our results are more comprehensive. Finally, two simulation results to prove the feasibility of theoretical derivation. Compared with integer-order MNNs, fractional-order MNNs have more complex dynamic behav-

ior and show stronger chaos. Therefore, the synchronization of fractional-order MNNs are our research direction in the future.

Acknowledgement: The authors would like to thanks the editor office for the deep advice to improve our work.

Funding Statement: This work was supported by National Natural Science Foundation of China under (Grant Nos. 62173175, 12026235, 12026234, 61903170, 11805091, 61877033, 61833005), and by 111 Project under Grant B17040, and by the Natural Science Foundation of Shandong Province under Grant Nos. ZR2019BF045, ZR2019MF021, ZR2019QF004, and by the Project of Shandong Province Higher Educational Science and Technology Program No. J18KA354, and by the Key Research and Development Project of Shandong Province of China, No. 2019GGX101003.

Conflicts of Interest: The authors declare that they have no conflicts of interest to report regarding the present study.

References

1. Chua, L. (1971). Memristor-the missing circuit element. *IEEE Transactions on Circuit Theory*, 18(5), 507–519. DOI 10.1109/TCT.1971.1083337.
2. Strukov, D. B., Snider, G. S., Stewart, D. R., Williams, R. S. (2008). The missing memristor found. *Nature*, 453(7191), 80–83. DOI 10.1038/nature06932.
3. Liu, W., Huang, J., Yao, Q. (2021). Stability analysis for quaternion-valued inertial memristor-based neural networks with time delays. *Neurocomputing*, 448, 67–81. DOI 10.1016/j.neucom.2021.03.106.
4. Sheng, Y., Huang, T., Zeng, Z., Li, P. (2021). Exponential stabilization of inertial memristive neural networks with multiple time delays. *IEEE Transactions on Cybernetics*, 51(2), 579–588. DOI 10.1109/TCYB.2019.2947859.
5. Shen, H., Hu, X., Wang, J., Cao, J., Qian, W. (2021). Non-fragile H_∞ synchronization for markov jump singularly perturbed coupled neural networks subject to double-layer switching regulation. *IEEE Transactions on Neural Networks and Learning Systems*, 1–11. DOI 10.1109/TNNLS.2021.3107607.
6. Gong, S., Guo, Z., Wen, S., Huang, T. (2021). Finite-time and fixed-time synchronization of coupled memristive neural networks with time delay. *IEEE Transactions on Cybernetics*, 51(6), 2944–2955. DOI 10.1109/TCYB.2019.2953236.
7. Kao, Y., Li, Y., Park, J. H., Chen, X. (2020). Mittag-leffler synchronization of delayed fractional memristor neural networks via adaptive control. *IEEE Transactions on Neural Networks and Learning Systems*, 32(5), 2279–2284. DOI 10.1109/TNNLS.2020.2995718.
8. Yuan, M., Wang, W., Wang, Z., Luo, X., Kurths, J. (2020). Exponential synchronization of delayed memristor-based uncertain complex-valued neural networks for image protection. *IEEE Transactions on Neural Networks and Learning Systems*, 32(1), 151–165. DOI 10.1109/TNNLS.5962385.
9. Wen, S., Zeng, Z., Huang, T., Zhang, Y. (2013). Exponential adaptive lag synchronization of memristive neural networks via fuzzy method and applications in pseudorandom number generators. *IEEE Transactions on Fuzzy Systems*, 22(6), 1704–1713. DOI 10.1109/TFUZZ.91.
10. Li, H., Fang, J. A., Li, X., Huang, T. (2020). Exponential synchronization of multiple impulsive discrete-time memristor-based neural networks with stochastic perturbations and time-varying delays. *Neurocomputing*, 392, 86–97. DOI 10.1016/j.neucom.2020.01.110.
11. Li, L., Xu, R., Gan, Q., Lin, J. (2020). A switching control for finite-time synchronization of memristor-based bam neural networks with stochastic disturbances. *Nonlinear Analysis: Modelling and Control*, 25(6), 958–979. DOI 10.15388/namc.2020.25.20557.

12. Wang, W., Jia, X., Wang, Z., Luo, X., Li, L. et al. (2020). Fixed-time synchronization of fractional order memristive mam neural networks by sliding mode control. *Neurocomputing*, 401, 364–376. DOI 10.1016/j.neucom.2020.03.043.
13. Li, S., Ahn, C. K., Xiang, Z. (2020). Command-filter-based adaptive fuzzy finite-time control for switched nonlinear systems using state-dependent switching method. *IEEE Transactions on Fuzzy Systems*, 29(4), 833–845. DOI 10.1109/TFUZZ.2020.2965917.
14. Cai, M., Xiang, Z. (2017). Adaptive practical finite-time stabilization for uncertain nonstrict feedback nonlinear systems with input nonlinearity. *IEEE Transactions on Systems, Man, and Cybernetics: Systems*, 47(7), 1668–1678. DOI 10.1109/TSMC.2017.2660761.
15. Hua, L., Zhu, H., Shi, K., Zhong, S., Tang, Y. et al. (2021). Novel finite-time reliable control design for memristor-based inertial neural networks with mixed time-varying delays. *IEEE Transactions on Circuits and Systems I: Regular Papers*, 68(4), 1599–1609. DOI 10.1109/TCSI.8919.
16. Shi, Y., Cao, J. (2020). Finite-time synchronization of memristive cohen–grossberg neural networks with time delays. *Neurocomputing*, 377, 159–167. DOI 10.1016/j.neucom.2019.10.036.
17. Polyakov, A. (2011). Nonlinear feedback design for fixed-time stabilization of linear control systems. *IEEE Transactions on Automatic Control*, 57(8), 2106–2110. DOI 10.1109/TAC.2011.2179869.
18. Li, N., Wu, X., Feng, J., Lü, J. (2020). Fixed-time synchronization of complex dynamical networks: A novel and economical mechanism. *IEEE Transactions on Cybernetics*, 1–11. DOI 10.1109/TCYB.2020.3026996.
19. Li, N., Wu, X., Feng, J., Xu, Y., Lü, J. (2020). Fixed-time synchronization of coupled neural networks with discontinuous activation and mismatched parameters. *IEEE Transactions on Neural Networks and Learning Systems*, 32(6), 2470–2482. DOI 10.1109/TNNLS.2020.3005945.
20. Ren, H., Peng, Z., Gu, Y. (2020). Fixed-time synchronization of stochastic memristor-based neural networks with adaptive control. *Neural Networks*, 130, 165–175. DOI 10.1016/j.neunet.2020.07.002.
21. Feng, L., Hu, C., Yu, J., Jiang, H., Wen, S. (2021). Fixed-time synchronization of coupled memristive complex-valued neural networks. *Chaos, Solitons & Fractals*, 148, 110993. DOI 10.1016/j.chaos.2021.110993.
22. Peng, T., Qiu, J., Lu, J., Tu, Z., Cao, J. (2021). Finite-time and fixed-time synchronization of quaternion-valued neural networks with/without mixed delays: An improved one-norm method. *IEEE Transactions on Neural Networks and Learning Systems*, pp. 1–13. DOI 10.1109/TNNLS.2021.3085253.
23. Wang, J., Huang, Z., Wu, Z., Cao, J., Shen, H. (2020). Extended dissipative control for singularly perturbed pdt switched systems and its application. *IEEE Transactions on Circuits and Systems I: Regular Papers*, 67(12), 5281–5289. DOI 10.1109/TCSI.8919.
24. Wang, J., Yang, C., Xia, J., Wu, Z. G., Shen, H. (2021). Observer-based sliding mode control for networked fuzzy singularly perturbed systems under weighted try-once-discard protocol. *IEEE Transactions on Fuzzy Systems*, pp. 1889–1899. DOI 10.1109/TFUZZ.2021.3070125.
25. Xiao, J., Zeng, Z., Wu, A., Wen, S. (2020). Fixed-time synchronization of delayed cohen–grossberg neural networks based on a novel sliding mode. *Neural Networks*, 128, 1–12. DOI 10.1016/j.neunet.2020.04.020.
26. Bao, Y., Zhang, Y., Zhang, B. (2021). Fixed-time synchronization of coupled memristive neural networks via event-triggered control. *Applied Mathematics and Computation*, 411, 126542. DOI 10.1016/j.amc.2021.126542.
27. Li, Y., Luo, B., Liu, D., Yang, Z., Zhu, Y. (2020). Adaptive synchronization of memristor-based neural networks with discontinuous activations. *Neurocomputing*, 381, 196–206. DOI 10.1016/j.neucom.2019.11.018.
28. Li, S., Peng, X., Tang, Y., Shi, Y. (2018). Finite-time synchronization of time-delayed neural networks with unknown parameters via adaptive control. *Neurocomputing*, 308, 65–74. DOI 10.1016/j.neucom.2018.04.053.
29. Filippov, A. F. (1988). *Differential equations with discontinuous righthand sides*. Dordrecht, The Netherlands: Springer.
30. Cao, J., Li, R. (2017). Fixed-time synchronization of delayed memristor-based recurrent neural networks. *Science China Information Sciences*, 60(3), 032201. DOI 10.1007/s11432-016-0555-2.
31. Parsegov, S., Polyakov, A., Shcherbakov, P. (2012). Nonlinear fixed-time control protocol for uniform allocation of agents on a segment. *Proceedings of 2012 IEEE 51st IEEE Conference on Decision and Control (CDC)*, pp. 7732–7737. New York. DOI 10.1109/CDC.2012.6426570.

32. Hardy, G. H., Littlewood, J. E., Pólya, G., Pólya, G. (1952). *Inequalities*. Cambridge, UK: Cambridge University Press.
33. Chen, J., Zeng, Z., Jiang, P. (2014). Global mittag-leffler stability and synchronization of memristor-based fractional-order neural networks. *Neural Networks*, 51, 1–8. DOI 10.1016/j.neunet.2013.11.016.